Experimental section

Materials

9H-carbazole, cholesterol chloroformate, Et_3N and Na_2SO_4 were purchased from Energy Chemical Company. Solvents were purchased from Xilong Chemical Co., Ltd. All the chemicals were used as received without further purification.

Instruments and methods

^1H and ^{13}C NMR spectra were recorded on a VNMRS 400 NMR spectrometer (Varian, USA). High resolution mass spectra (HR-MS) were recorded using an Autoflex III mass spectrometer (MALDI-TOF-MS, Bruker, Germany). Element analysis was performed using a vario EL cube elemental analyzer (Elementar, Germany). UV-Vis spectra were recorded using a UV-2600 spectrometer (Shimadzu, Japan). UV-Vis reflection spectra were recorded using a UV-2600 spectrometer with accessory ISR-2600Plus. Absolute quantum efficiency was measured on an integrating sphere (C11347-11, Hamamatsu, Japan). Fluorescence lifetime was measured on a compact fluorescence lifetime spectrometer (C11367-11, Hamamatsu, Japan). Sample heating was performed on a microcomputer temp-controlled heating board (JF-966A, JFTOOLS, China). DSC measurements were carried out on a NETZSCH DSC 200F3 instrument at a heating rate and a cooling rate of 10 ^{o}C min^{-1} in nitrogen. TGA analysis was performed on a NETZSCH SA409PC thermogravimeter. Powder X-ray diffraction (PXRD) patterns were carried out in the reflection mode at room temperature using a 2.2 kW Empyrean X-ray Diffraction System (PANalytical, Netherland). Photos and Video were taken by Nikon D7100. High-performance liquid chromatogram (HPLC) curves were recorded using an Agilent 1260 Infinity Ⅱ (QA&QC-HPLC-19) by DAICELCHIRALTECHNOLOGIES(CHINA) CO., LTD.

Computational Details

To simulate solid-state effects in crystal, the quantum mechanics and molecular mechanics (QM/MM) model with two-layer ONIOM method was built as shown in Figure S9. The central molecule was chosen as QM region, while the surrounding molecules were chosen as frozen MM part. The equilibrium structures of ground and triplet states (T_1) were optimized by using (U)M06/6-31G(d). Based on the T_1-geometry, the vertical excitation energies and natural transition orbitals (NTOs) of the low-lying excited states were carried out at the TD-M06/6-31G(d) level. All the above calculations were performed by Gaussian 09 package[1]. At the same level, the spin-orbit coupling matrix elements between singlet ant triplet states were also calculated by PySOC code.[2]

The three dyes were synthesized according to reported document.[3]

^{1}H NMR of Dye G. ^1H NMR (400 MHz, DMSO): δ = 7.78 (d, J = 7.2 Hz, 4H), 7.51 (d, J = 6.8 Hz, 4H), 7.38 – 7.22 (m, 12H), 7.11 (d, J = 6.8 Hz, 4H) ppm.

^{1}H NMR of Dye Y. ^{1}H NMR (400 MHz, $CDCl_3$): δ = 7.96 (d, J = 6.8 Hz, 2H), 7.89 (d, J = 8.8 Hz, 2H), 7.79 – 7.75 (m, 2H), 7.55 (t, J = 7.2 Hz, 2H), 7.46 (t, J = 7.2 Hz, 1H), 7.30 (m, 4H), 7.21 (m, 6H), 7.07 (t, J = 7.2 Hz, 2H) ppm.

^{1}H NMR of Dye R. ^{1}H NMR (400 MHz, $CDCl_3$): δ = 10.12 (s, 1H), 8.17 (d, J = 8.4 Hz, 2H), 8.06 (d, J = 8.0 Hz, 2H), 7.90 (d, J = 8.8 Hz, 2H), 7.86 (d, J = 7.6 Hz, 1H), 7.80 (d, J = 7.6 Hz, 1H), 7.31 (t, J = 8.4 Hz, 4H), 7.21 (t, J = 8.8 Hz, 6H), 7.09 (t, J = 7.2 Hz, 2H) ppm.

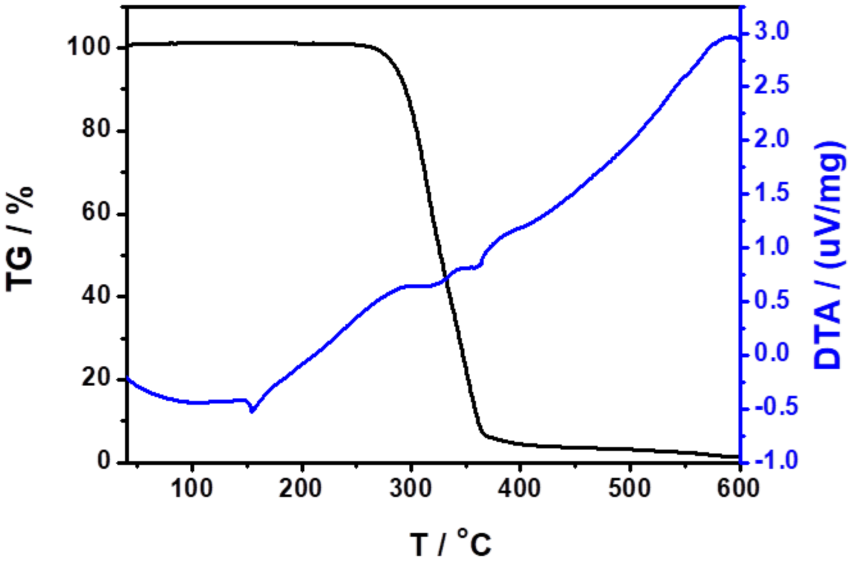

Figure S1. Thermogravimetric and DTA curves of compound **1**.

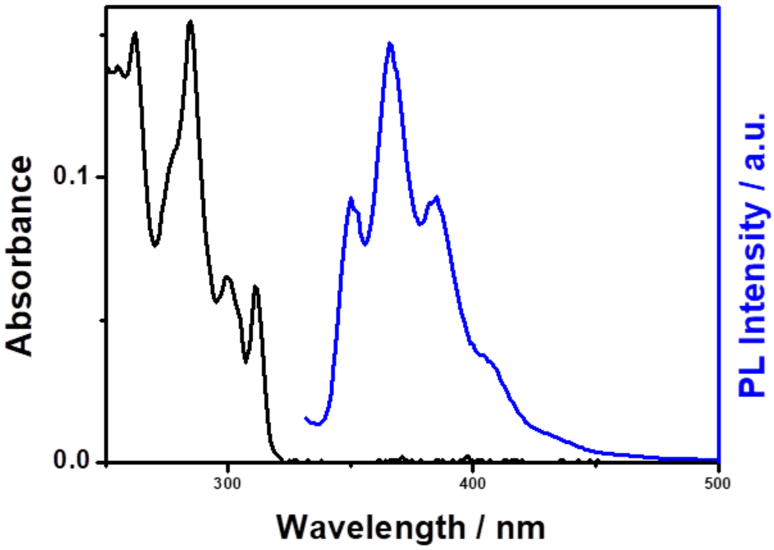

Figure S2. Absorption and fluorescence spectra of **1** in THF solution (10 μM).

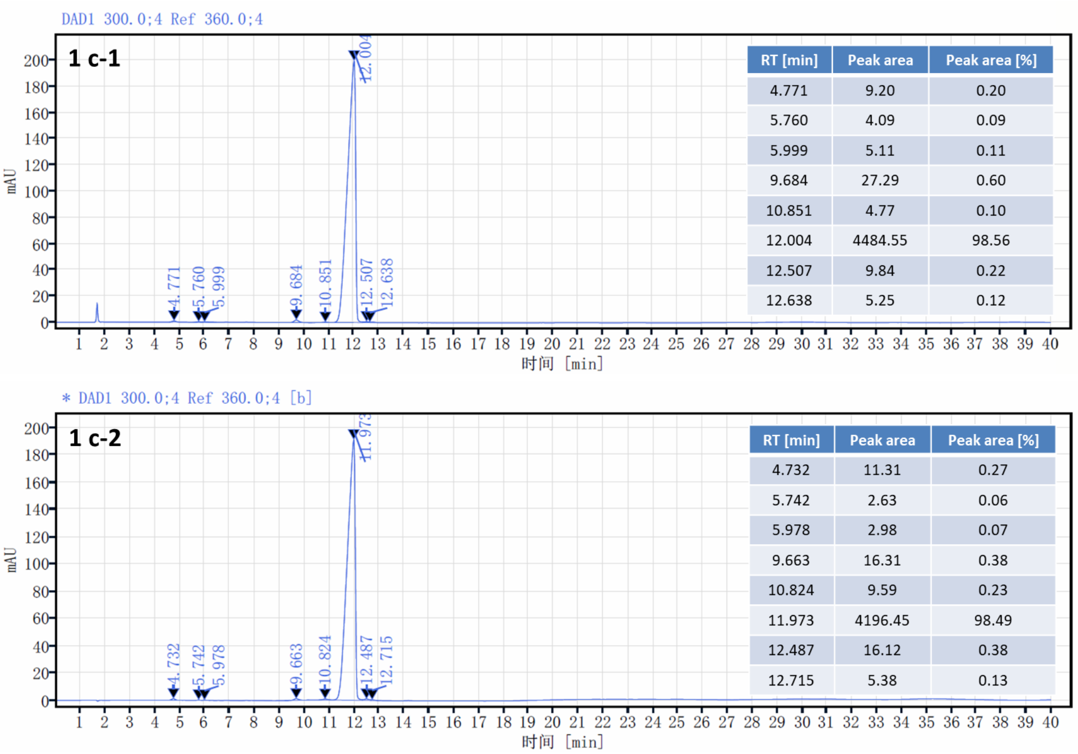

1 c-1

RT [min]	Peak area	Peak area [%]
4.771	9.20	0.20
5.760	4.09	0.09
5.999	5.11	0.11
9.684	27.29	0.60
10.851	4.77	0.10
12.004	4484.55	98.56
12.507	9.84	0.22
12.638	5.25	0.12

1 c-2

RT [min]	Peak area	Peak area [%]
4.732	11.31	0.27
5.742	2.63	0.06
5.978	2.98	0.07
9.663	16.31	0.38
10.824	9.59	0.23
11.973	4196.45	98.49
12.487	16.12	0.38
12.715	5.38	0.13

Column	Water Xbridge Phenyl 0.46 cm I.D. ×15 cm L, 3.5μm
Injection	5μl
Mobile phase	B：ACN(0.05%TFA)；A：H2O(0.05%TFA)(v/v)
Gradient	B/A=90/10 (v/v)
Flow rate	1.0ml/min
Wavelength	UV300nm
Temperature	40℃
Sample solution	1.0 mg/ml in THF70% ACN30%
HPLC equipment	Agilent 1260 Infinity Ⅱ QA&QC-HPLC-19

Figure S3. HPLC curves of **1c-1** and **1c-2** in acetonitrile/H_2O solution and the test parameters.

Table S1. Optical properties of compound **1** in various solid forms.

form	λ_{em}[nm]^a	Φ_{fl}[%]^b	Φ_{phos}[%]^c	τ[ns]^d
1o	385	33.82	_	6.500
1g	385	29.26	_	6.359
1h	385	27.62	0.18	6.041
1c-1	390	18.96	1.54	6.138
1c-2	385	50.19	_	6.893

[a]Emission maximum. [b]Fluorescence quantum yield determined by using a calibrated integrating sphere. [c]RTP quantum yield determined by using a calibrated integrating sphere. [d]Fluorescence lifetime.

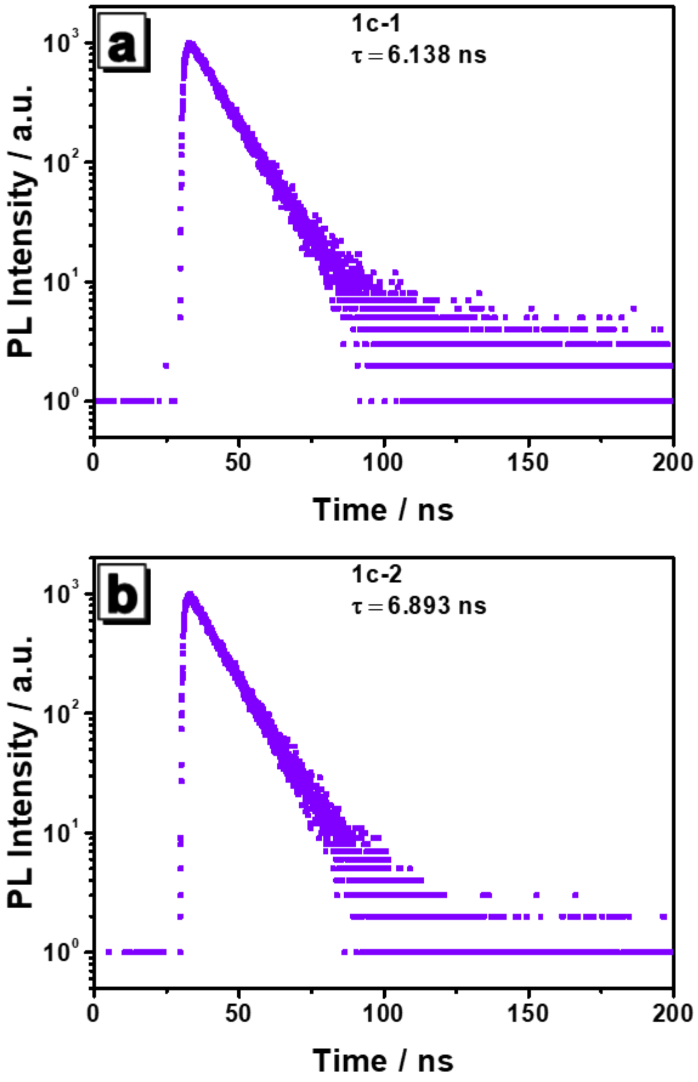

Figure S4. Decay curves of the fluorescence of (a) **1c-1** and (b) **1c-2**.

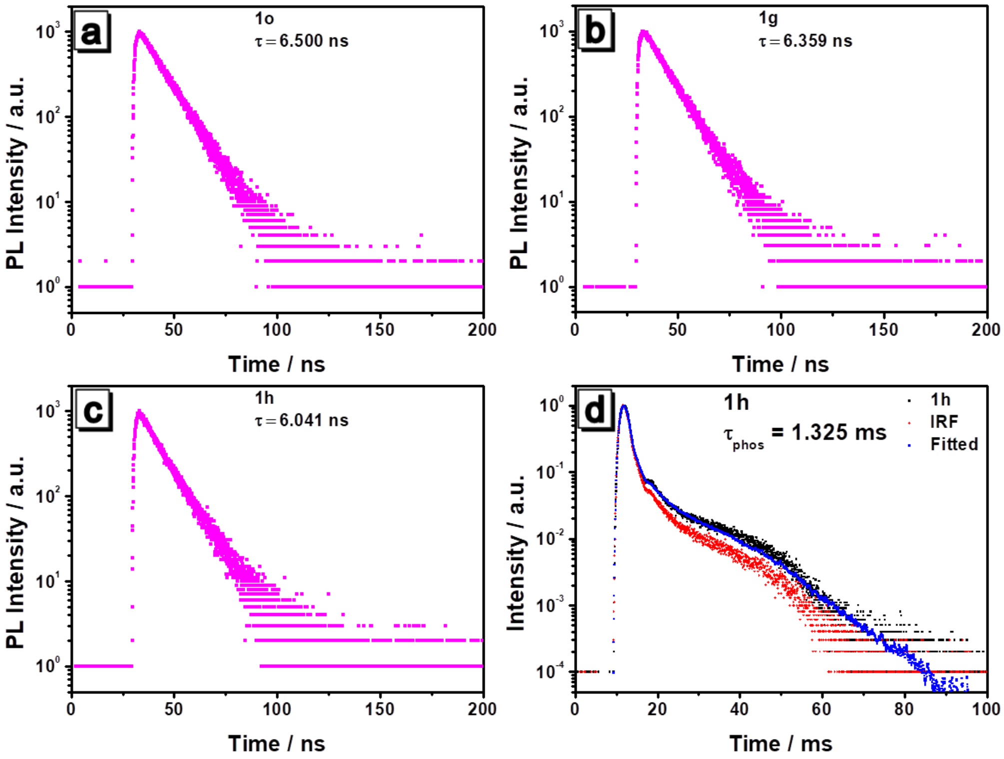

Figure S5. Decay curves of the fluorescence of (a) **1o**, (b) **1g** and (c) **1h**. (d) Decay curves of the RTP of **1h**.

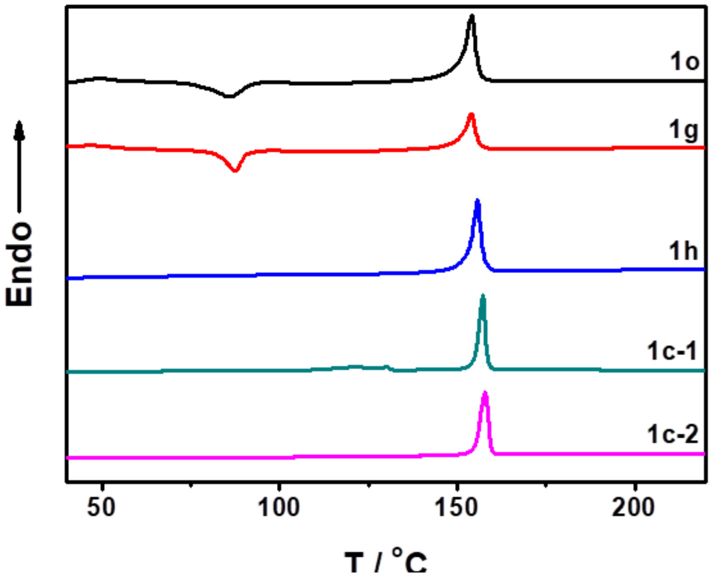

Figure S6. DSC curves of all the powders and single crystals of **1**.

Table S2. Single crystal data of **1c-1** and **1c-2**.

CCDC number	1972037	2018617
	1c-1	**1c-2**
formula	$C_{40}H_{53}NO_2$	$C_{40}H_{53}NO_2$
formula Weight /g•mol^{-1}	579.83	579.83
crystal system	monoclinic	triclinic
space group	C_2	P_1
T/K	150	100
Z	4	4
a/Å	19.8231(7)	14.8060(7)
b/Å	7.5996(2)	15.4949(7)
c/Å	24.2836(8)	17.2480(8)
α/°	90	111.3480(10)
β/°	112.008(4)	112.1740(10)
γ/°	90	85.3590(10)
V/Å^3	3391.7(2)	3288.5(3)
ρ_c/g•cm^{-3}	1.135	1.171
μ/mm^{-1}	0.520	0.07
F(000)	1264.0	1264.0
Reflections collected	8743	112219
Independent reflections	5093	30227
R_{int}	0.0311	0.0338
$R_1(I > 2\sigma(I))$	0.0727	0.0411
wR_2	0.2171	0.1013
GOOF	1.085	1.014

Table S3. Summary of the intermolecular interactions in **1c-1** and **1c-2**.

crystal	**1c-1**				**1c-2**
conformation	**Form I**	**Form II**	**Form III**	**Form IV**	
	d / Å	d / Å	d / Å	d / Å	d / Å
C-H···O	2.604(1)[a]	2.666(1)	2.666(1)	2.604(1)	2.672(2)
	2.863(1)	2.723(1)	2.723(1)	2.777(1)	2.728(2)
	2.981(1)	2.780(1)	2.777(1)	2.863(1)	2.811(2)
	2.994(1)	2.788(1)	2.780(1)	2.915(1)	3.117(2)
	3.057(1)	3.050(1)	2.788(1)	2.942(1)	
	3.180(1)	3.180(1)	2.915(1)	3.050(1)	
			2.942(1)	3.057(1)	
			2.981(1)	3.060(1)	
			2.994(1)	3.185(1)	
			3.060(1)		
			3.185(1)		
C-H···N					2.979(2)
C-H···π[b]	2.810(1)	2.934(1)	2.810(1)	3.100(1)	2.860(2)
	2.927(1)	3.100(1)	2.927(1)	3.150(1)	3.004(2)
	2.934(1)		3.019(1)		3.022(2)
	3.019(1)		3.150(1)		3.110(2)
C-H···H-C					1.922(2)
					1.926(1)
π-π[c]	3.361(1)	3.293(1)	3.330(1)	3.361(1)	

a) The number of hydrogen bonds; b) Bond length of C-H···π interaction is the distance between hydrogen atom and the plane of aromatic ring; c) due to the existence of small dihedral angle between carbazole moieties, distance of π-π interaction is defined as distance between centroid of one aromatic ring and plane of the other aromatic ring.

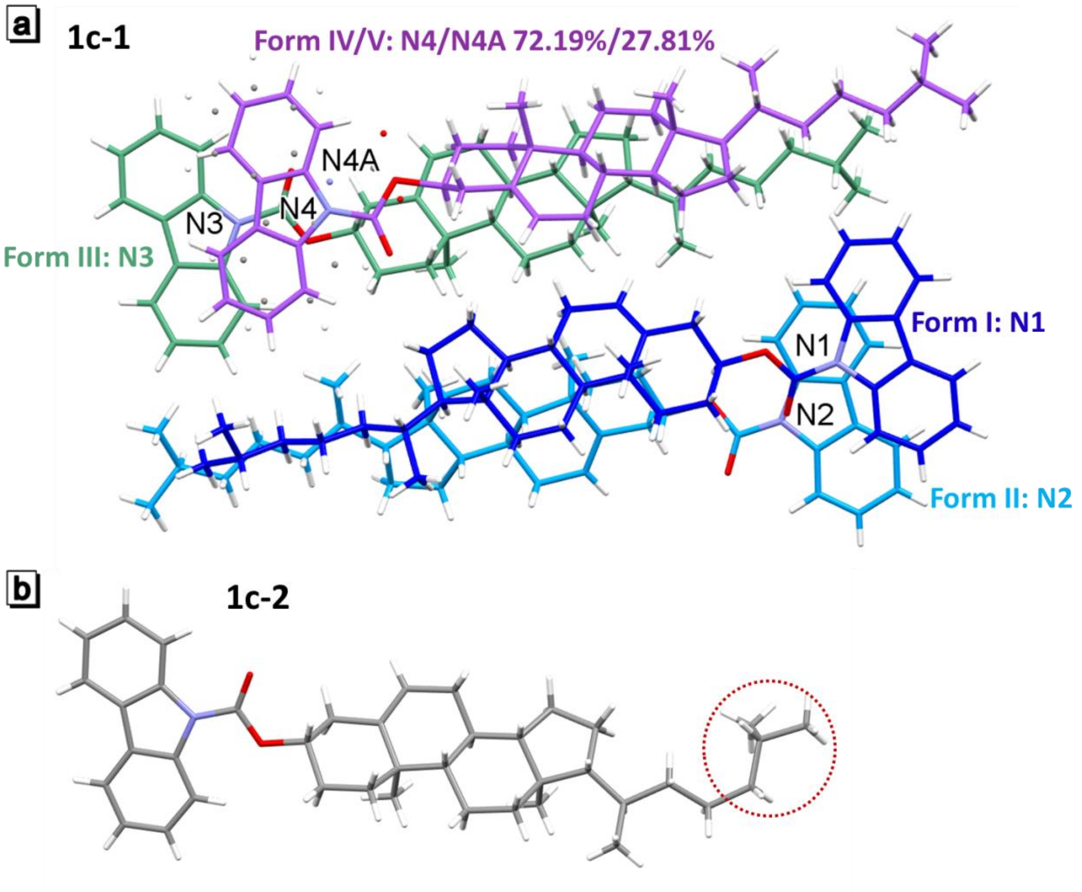

Figure S7. X-ray crystal structure of single crystal (a) **1c-1** and (b) **1c-2**.

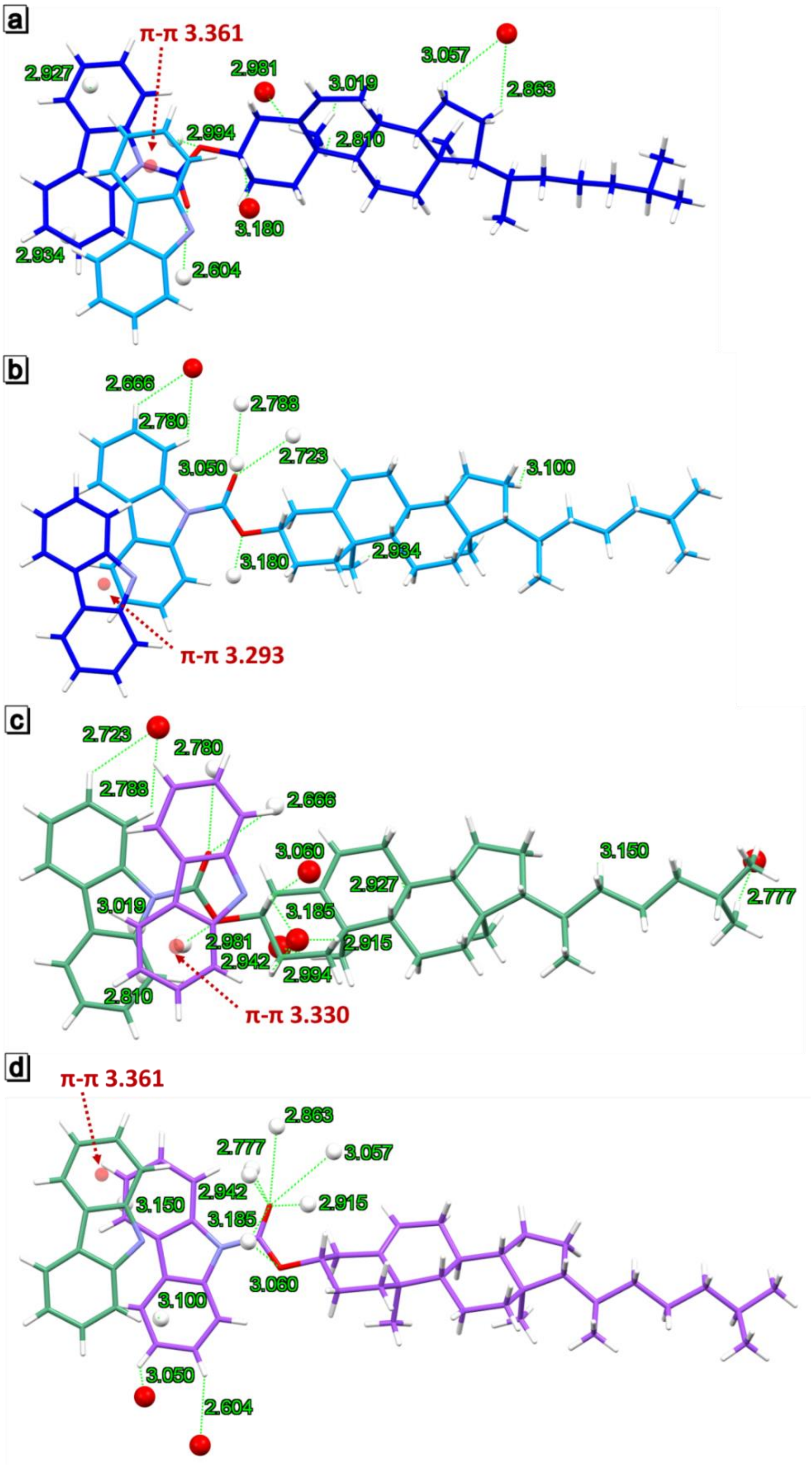

Figure S8. The detailed intermolecular interactions of (a) form I, (b) form II, (c) form III and (d) form IV in single crystal **1c-2**. Bond length of C-H···π interaction is the distance between hydrogen atom and the plane of aromatic ring. Centroids of aromatic rings are shown in red. Due to the existence of small dihedral angle between adjacent carbazole moieties, distance of π-π interaction is defined as distance between centroid of one aromatic ring and the plane of the other aromatic ring.

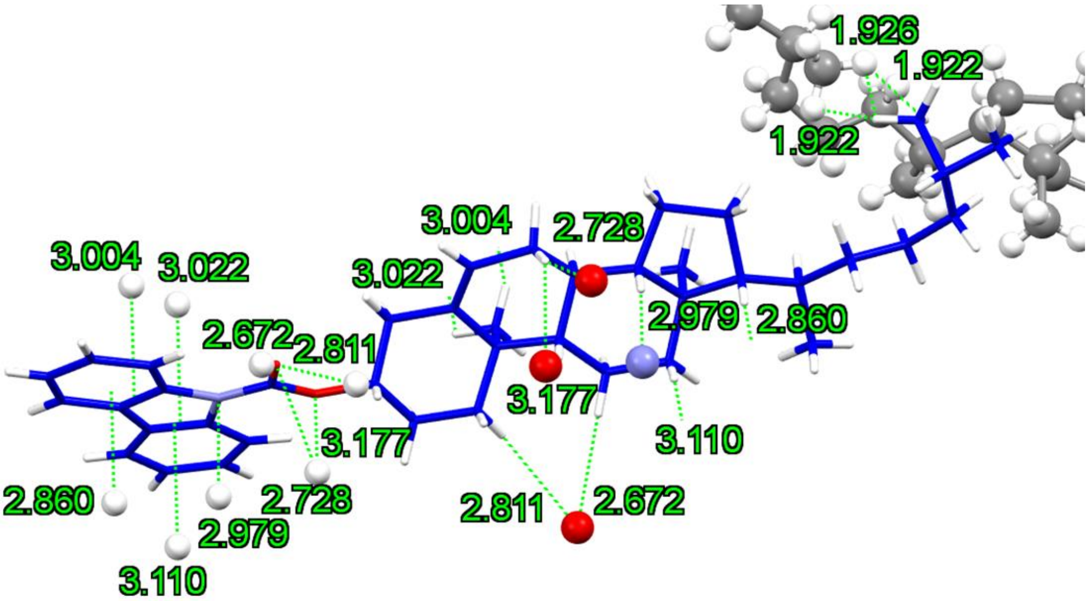

Figure S9. The detailed intermolecular interactions in single crystal **1c-1**. Bond length of C-H···π interaction is the distance between hydrogen atom and the plane of aromatic ring.

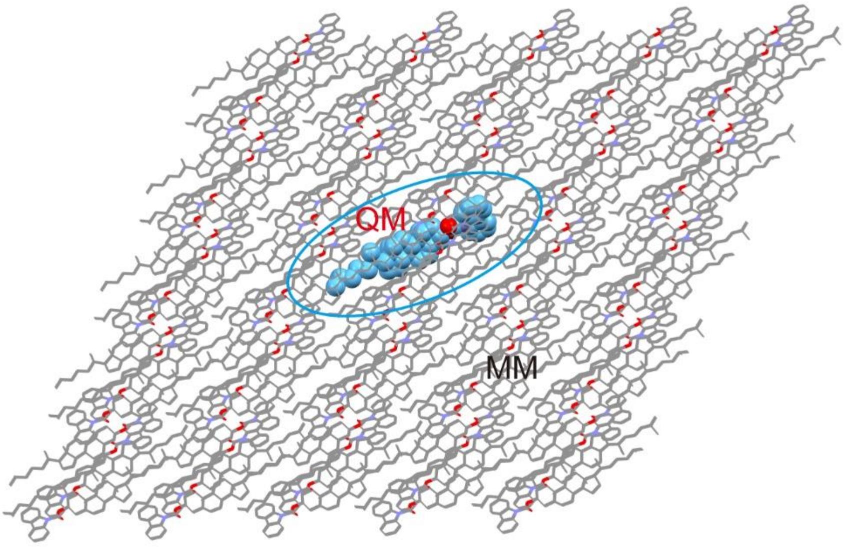

Figure S10. Set up of QM/MM model, taking **1c-1** as example. Note that the hydrogen atoms are omitted for clarity.

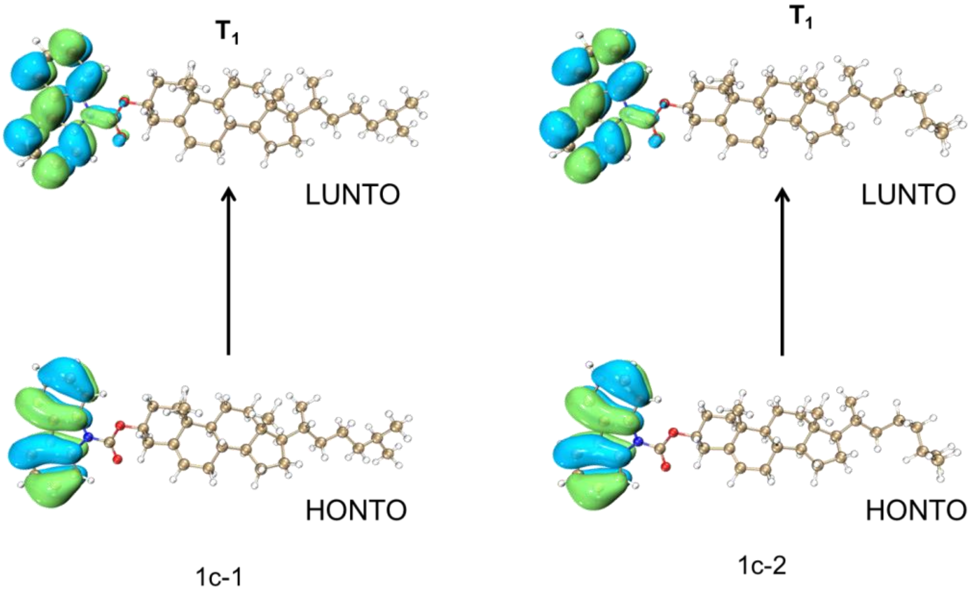

Figure S11. Natural transition orbtials (NTOs) of T$_1$ states for **1c-1** and **1c-2**.

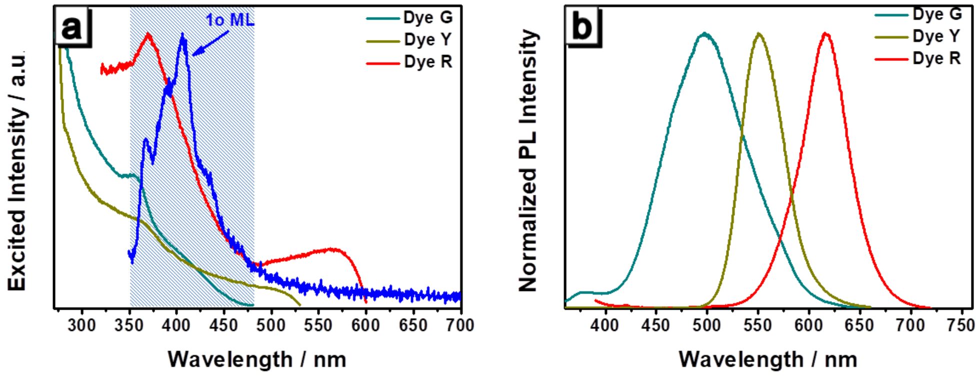

Figure S12. (a) Solid state excited spectra of different dyes and ML spectra of **1o**. (b) Fluorescence spectra of different dyes.

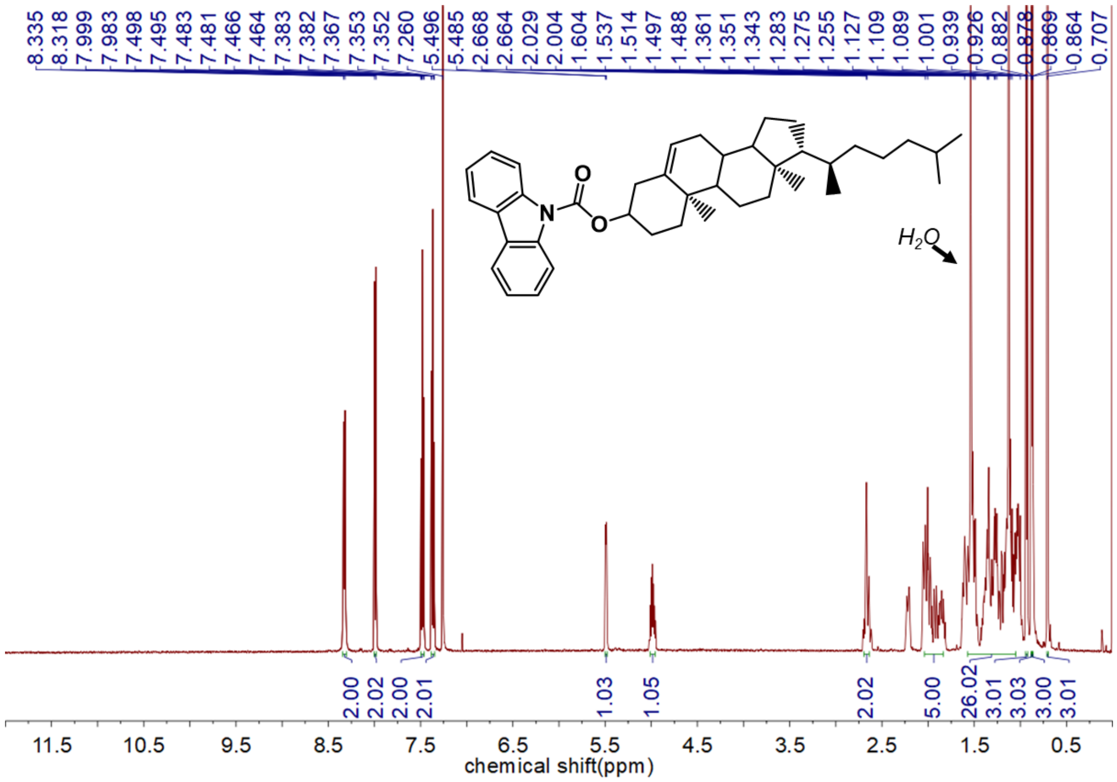

Figure S13. ^{1}H NMR of compound **1**.

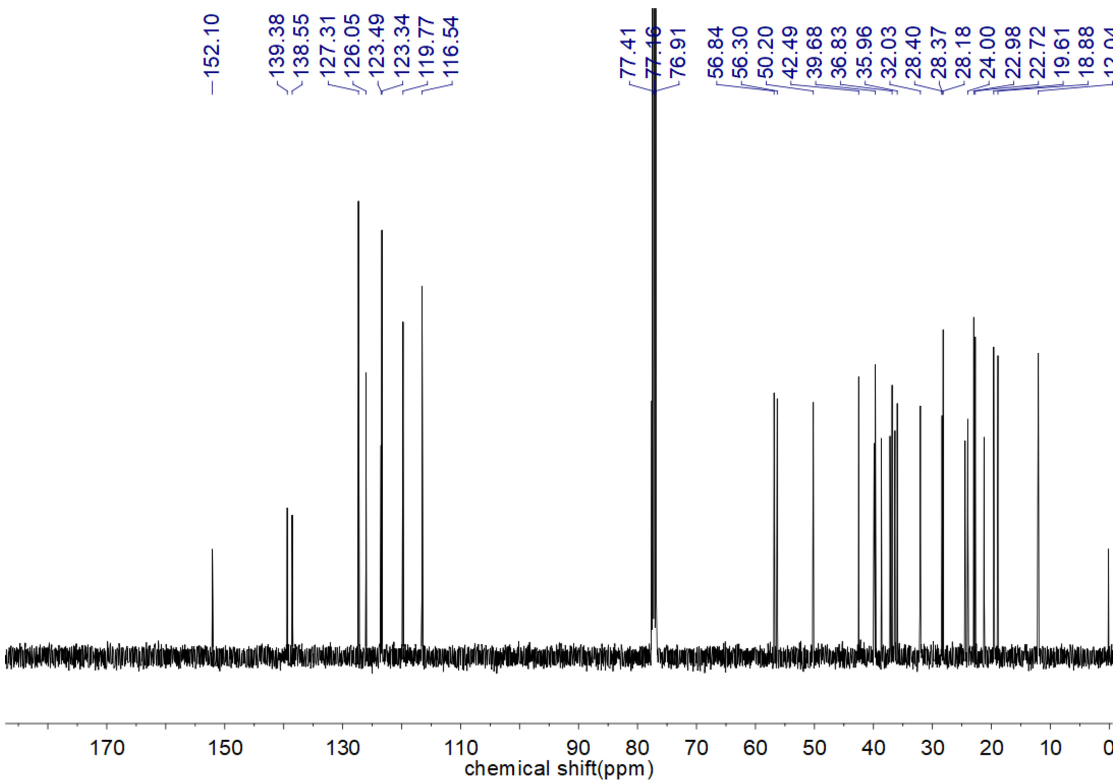

Figure S14. ^{13}C NMR of compound **1**.

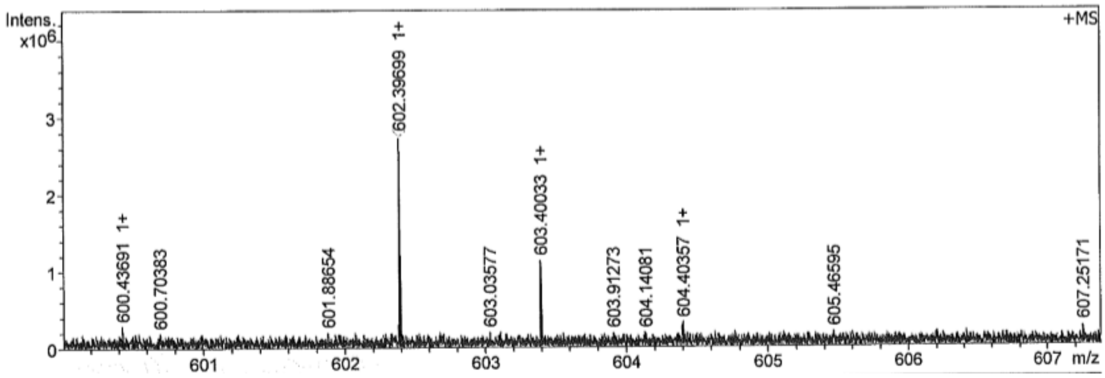

Figure S15. HRMS of compound 1.

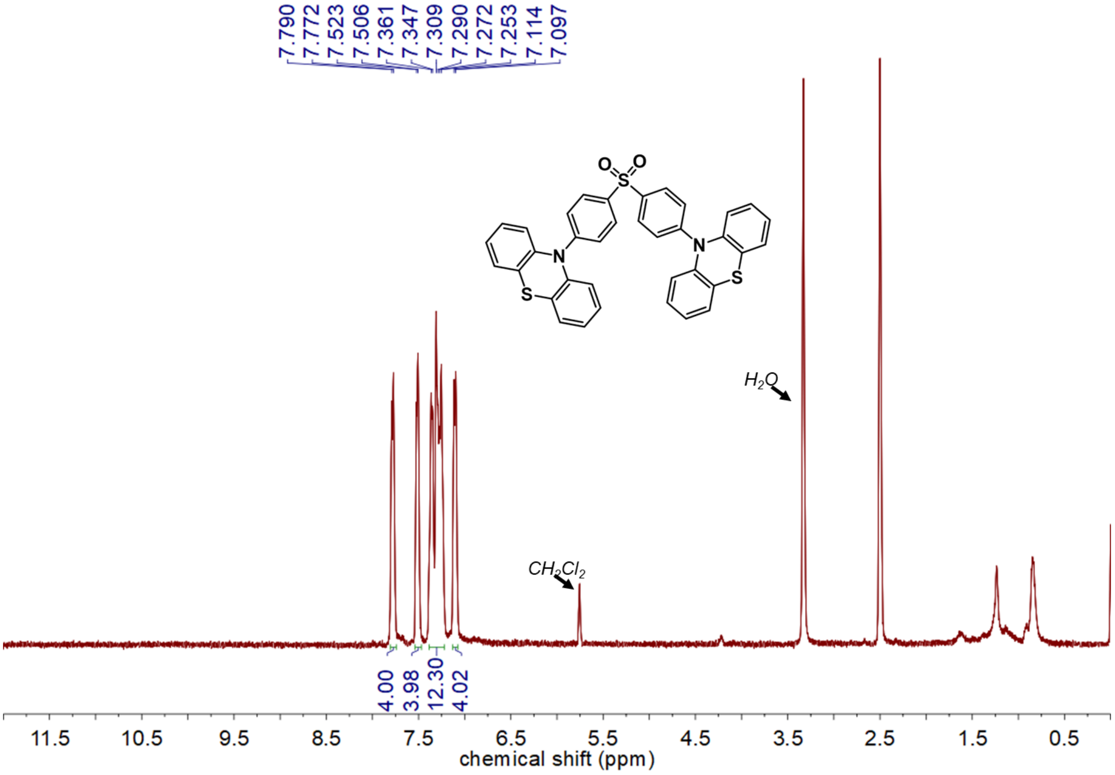

Figure S16. ^{1}H NMR of Dye G.

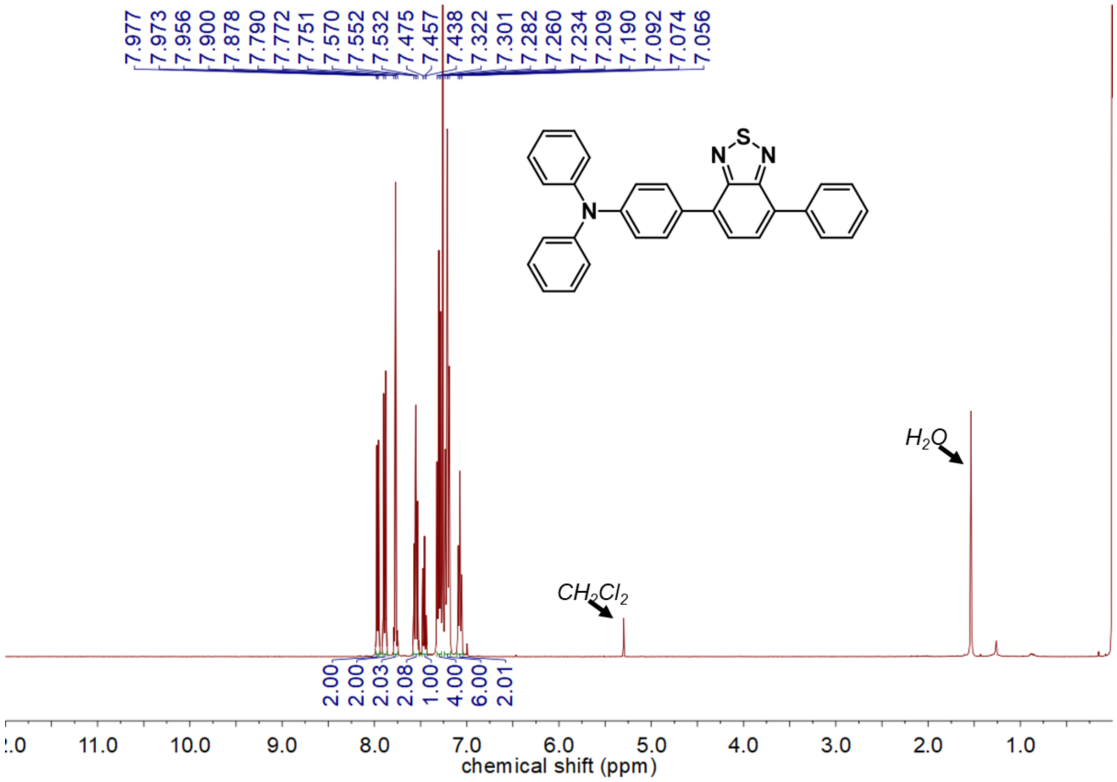

Figure S17. ^1H NMR of Dye Y.

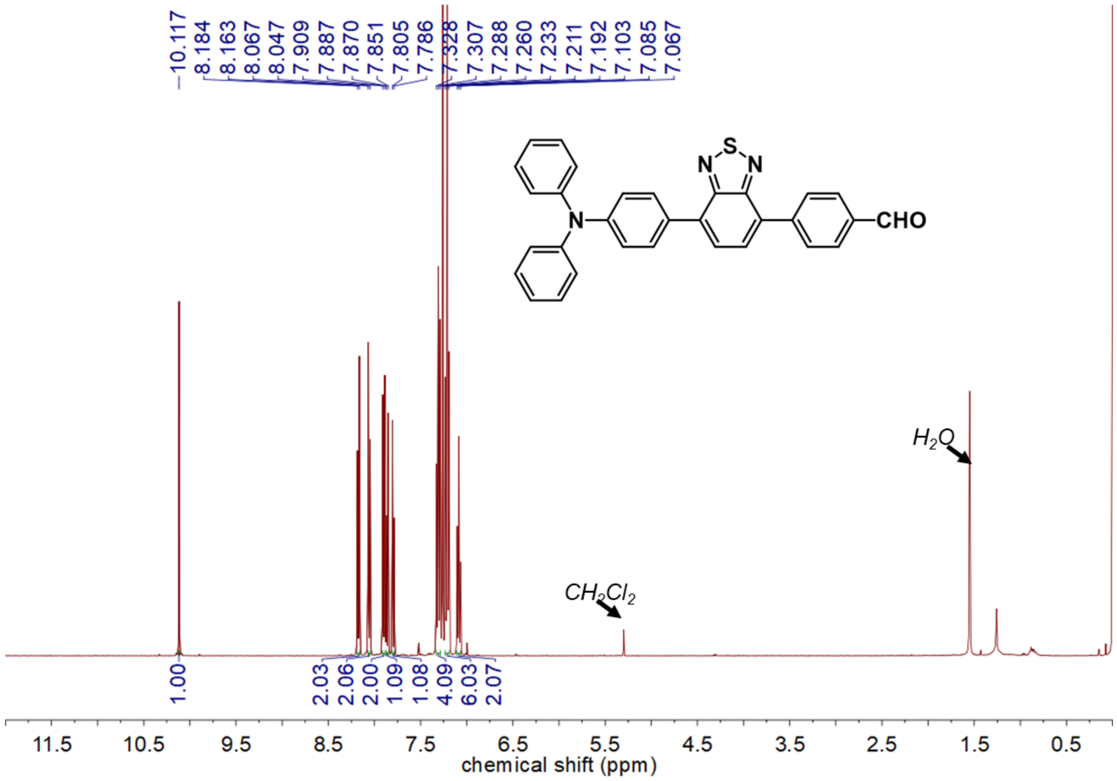

Figure S18. ^1H NMR of Dye R.

References

1. Frisch, M. J.; Trucks, G. W.; Schlegel, H. B.; Scuseria, G. E.; Robb, M. A.; Cheeseman, J. R.; Scalmani, G.; Barone, V.; Mennucci, B.; Petersson, G. A.; Nakatsuji, H.; Caricato, M.; Li, X.; Hratchian, H. P.; Izmaylov, A. F.; Bloino, J.; Zheng, G.; Sonnenberg, J. L.; Hada, M.; Ehara, M.; Toyota, K.; Fukuda, R.; Hasegawa, J.; Ishida, M.; Nakajima, T.; Honda, Y.; Kitao, O.; Nakai, H.; Vreven, T.; Montgomery Jr., J. A.; Peralta, J. E.; Ogliaro, F.; Bearpark, M. J.; Heyd, J.; Brothers, E. N.; Kudin, K. N.; Staroverov, V. N.; Kobayashi, R.; Normand, J.; Raghavachari, K.; Rendell, A. P.; Burant, J. C.; Iyengar, S. S.; Tomasi, J.; Cossi, M.; Rega, N.; Millam, N. J.; Klene, M.; Knox, J. E.; Cross, J. B.; Bakken, V.; Adamo, C.; Jaramillo, J.; Gomperts, R.; Stratmann, R. E.; Yazyev, O.; Austin, A. J.; Cammi, R.; Pomelli, C.; Ochterski, J. W.; Martin, R. L.; Morokuma, K.; Zakrzewski, V. G.; Voth, G. A.; Salvador, P.; Dannenberg, J. J.; Dapprich, S.; Daniels, A. D.; Farkas; Foresman, J. B.; Ortiz, J. V.; Cioslowski, J.; Fox, D. J.; Gaussian 09, Revision D.01; Gaussian, Inc.: Wallingford, CT, 2013.

2. Gao, X.; Bai, S.; Fazzi, D.; Niehaus, T.; Barbatti, M.; Thiel, W. J. Chem., *Theory Comput.* 2017, 13, 515-524.

3. Wenlang Li, et al. *Angew. Chem. Int. Ed.* 2018, 57(39), 12727-12732.